

# A Flexible Architecture for Welding Simulators Used in Weld Planning

## Authors

Jeberg P. V., /Department of Technology Development, Odense Steel Shipyard (Denmark) /M.Sc.

Cai X., /Simula Research Laboratory (Norway) /Assoc. Professor, Ph.D.

Holm H., /Department of Production, Aalborg University (Denmark) /Professor, Ph.D.

Langtangen H. P., /Simula Research Laboratory (Norway) /Professor, Ph.D.

## Keywords

**Welding simulation, heat conduction, weld pool surface deformation, finite elements, object-oriented programming**

## Abstract

This paper presents a general architecture for welding simulation systems, which can be used to simulate features such as heat conduction, weld pool surface deformation, material addition and different couplings between them. The architecture consists of individual modules that handle different welding features, so it is easy to configure a particular welding application. The overall numerical strategy behind the architecture is based on two modules. The first module handles a non-linear partial differential equation (PDE) describing the heat conduction in a 3D work piece, while the second module handles a system of two coupled non-linear PDEs modelling the weld pool surface deformation. Finite elements are used in the spatial discretisations and advanced non-linear solvers are used to achieve a stable and good numerical performance. The implementation of the architecture uses object-oriented programming techniques, enhancing the capability of configuring different welding applications. To demonstrate its functionality, the architecture is applied to a vertical I-joint gas metal arc welding simulation.

# 1 Introduction

During the last decade, the European ship-building industry has experienced a severe competition, which has resulted in an ongoing struggle to increase the efficiency of the production. One of the areas of interest is the welding process. Along with increasing computer power, simulation has been increasingly used to obtain insight into the welding process. Simulation is used to design welding procedures, both for assisting human welders and for automation of robotic weld planning and programming. However, different welding applications require different simulation functions and, thereby, different configurations of the simulation systems.

Most welding simulations are limited to simulating temperature distribution in work pieces, see e.g. [2]. But temperature distribution is also of interest for identifying the weld pool size, which influences the penetration, and for identifying the thermal history, which influences the microstructure in the metal and the distortion of the work piece; properties of great importance for the industrial production. In addition, welding simulation may also incorporate the addition of material to be able to model welding processes like gas metal arc welding (GMAW) more precisely, see e.g. [5].

Several research papers [1, 11, 14] have reported the use of a two-dimensional weld pool surface model to account for the deformation of the weld pool surface. This is of special interest for postural welding, because of the influence of gravity on the molten metal in the weld pool and thereby the weld pool surface deformation.

These two different simulation systems can provide different simulation capabilities and will, therefore, be useful for different types of welding applications. To the knowledge of the authors, no attempt has been reported to generalise the architectures of these different simulation systems to achieve a systematic approach to a flexible configuration of different simulation systems.

Therefore, a general architecture is suggested in the present study. This paper presents the architecture and associated configurations of different welding applications. The architecture is implemented using Diffpack [3, 9], which is a scientific-computing environment with an emphasis on the finite element method. The used object-oriented programming style has enabled the implementation of individual modules for different welding features. These modules are easily extensible, therefore of great interest to an ongoing project to develop an automated off-line programming system for posture robot welding at Odense Steel Shipyard Ltd. and at Department of Production, Aalborg University. This off-line programming system bases the programming of the robots on simulated trajectories of the control variables, e.g., position and velocity of the weld gun, voltage and wire feed speed [7]. As a concrete example for this paper, the architecture is used to configure a simulation system for vertical single pass I-joint GMAW. The numerical approach and some obtained results are reported.

## 2 A general architecture

When building welding simulation systems and, hence, choosing appropriate numerical models of the welding process, it is important to know in which context the models are used. This is of importance because different phenomena are of different importance in different applications. A main objective in the modelling process is to identify the most important phenomena related to the application. This is done to keep the complexity of the model as low as possible, but still obtain a sufficient model agreement with reality to fulfil application requirements. Therefore, a modelling process can be iterative to obtain a simple and useful model.

The most important phenomenon in welding is heat conduction, which determines the thermal history of the work piece and, hence, the course of the fusion of the base material. The thermal history has also a large impact on the microstructure in the metal and on the work piece deformation. For these reasons, a heat conduction model is mandatory for a welding simulation system. However, several phenomena are present in a convective flow of liquid metal in the weld pool, which entail energy dissipation and thereby influence the shape of the weld pool and, hence, the fusion and penetration of the work piece. At the present stage of the development of the simulation system presented in this paper, the convective flow of liquid is not included in the model. Instead the energy dissipation is accounted for by a three-dimensional heat distribution [4]. This simplification is introduced because it is assumed that the improved accuracy of the shape of the weld pool, which can be obtained by accounting for the effects causing the convective flow of liquid, does not justify the increased development expense. In this way, the important effect of energy dissipation has been accounted for by a relatively simple mathematical model, which preserves model simplicity.

In addition to disregarding the phenomenon that causes the convective flow of liquid in the weld pool, the dynamical deformation of the weld pool surfaces is also excluded at the present stage. The weld pool surface deformation is not regarded important in top-down welding without either material addition or full penetration, because the weld pool bed can support the liquid metal. Therefore, there is a very limited risk that liquid metal will leave the weld seam and cause a destroyed weld process. However, in postural welding, the surface deformation becomes important because this risk increases. Instead of a complex dynamical model, a simplified static model can be used to model gravity and arc pressure on the weld pool surface deformation [11]. Moreover, if welding processes with addition of material are modelled, this effect should also be included to account for the effect of work piece reinforcement.

In the light of the above description of the context in which the welding process model is to be used, a general architecture for a welding simulation system should consist of four different modules. The modules should allow different configurations of the coupling between them, such that different welding applications can be handled properly. The four modules are:

- Heat conduction module.
- Surface deformation module.
- Free surface domain extraction module.
- Material addition module.

## 2.1 Heat conduction module

The heat conduction module calculates the three-dimensional temperature distribution in a work piece. It uses the Fourier heat conduction model described by the following non-linear PDE:

$$\rho c(u) \frac{\partial u}{\partial t} = \frac{\partial}{\partial x} \left( k(u) \frac{\partial u}{\partial x} \right) + \frac{\partial}{\partial y} \left( k(u) \frac{\partial u}{\partial y} \right) + \frac{\partial}{\partial z} \left( k(u) \frac{\partial u}{\partial z} \right) + Q_v'''(x, y, z, t) \quad \text{in } \Omega. \quad (1)$$

In the above equation,  $u$  is the primary unknown and represents temperature,  $\rho$  represents density,  $c(u)$  represents a specific heat capacity,  $k(u)$  represents the thermal conductivity for an isotropic material,  $t$  represents time,  $x, y, z$  represent space coordinates,  $Q_v'''$  represents internal energy generation per volume and  $\Omega$  represents the spatial domain of the work piece.

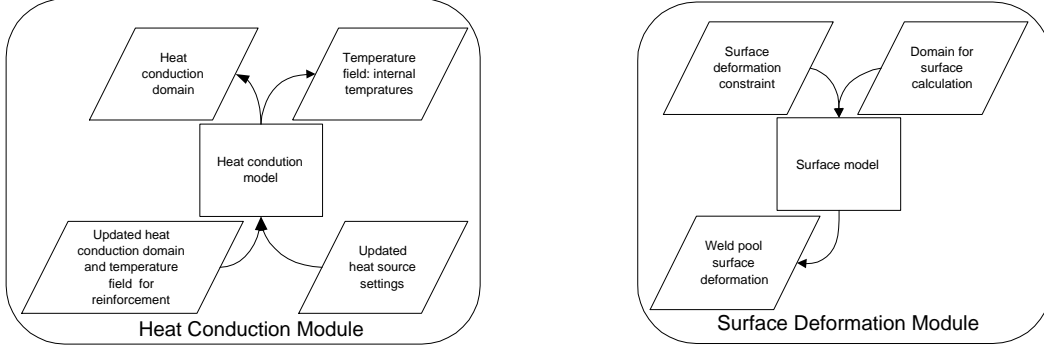


Figure 1: Left: A diagram of the heat conduction module with associated information input and output. Right: A diagram of the surface deformation module with associated information input and output.

On the surface of  $\Omega$ , the heat transport is determined by convection and radiation. Convection is dominating at some distance away from the weld pool, whereas radiation is dominant in the area of high temperature close to the weld pool. Therefore, the chosen boundary equation is as follows (see [10]):

$$-k(u) \frac{\partial u}{\partial n} = c_{\text{con}}(u - u_{\text{sur}}) + c_{\text{rad}}(u^4 - u_{\text{sur}}^4) \quad \text{on } \partial\Omega. \quad (2)$$

In the above equation,  $\frac{\partial u}{\partial n}$  represents the normal derivative of  $u$  on  $\partial\Omega$ ,  $c_{\text{con}}$  represents the convection factor,  $c_{\text{rad}}$  represents the radiation factor and  $u_{\text{sur}}$  represents the temperature of the surroundings.

The energy input from the heat source to the work piece channels through the surface of the weld pool. Here, the heat source refers to the welding torch and welding arc. The properties of the heat source include velocity, position, voltage, current, wire feed speed. Inside the weld pool, convective flow results in a dispersion of energy. To account for the energy dispersion, the energy input can be regarded as an internal energy generation instead of a boundary condition. On a flat work piece, the energy dispersion can be accounted for by a three-dimensional ellipsoidal energy distribution of the form [4]:

$$Q_v'''(x^*, y^*, z^*) = \frac{6\sqrt{3}fQ}{abc\pi\sqrt{\pi}} e^{-\left(\frac{3x^{*2}}{a^2} + \frac{3y^{*2}}{b^2} + \frac{3z^{*2}}{c^2}\right)}. \quad (3)$$

In the  $Q_v'''$  function,  $x^*, y^*, z^*$  represent space coordinates relative to the position of the heat source,  $Q$  represents the effective power (W) delivered by the heat source,  $a, b, c$  represent variables that control the extent of the heat source, and  $f$  represents a factor used to change the ellipsoidal shape in front of and behind the heat source.

Initially, the input to the heat conduction module is the three-dimensional geometry of a work piece to set up the domain. During the simulation, the module needs information on  $Q_v'''$ , position and speed of the heat source to calculate the influence on the temperature distribution.  $Q_v'''$  is calculated from voltage, current and wire feed speed. Additionally, the module may need an updated domain and temperature field to account for the change in the domain because of reinforcement. The primary output is the three-dimensional temperature field  $u$ , which gives the internal temperature distribution in the work piece. The output may also include an updated  $\Omega$  in case it is needed for reinforcement update. The left picture of Figure 1 shows a diagram of the heat conduction module with information input and output during a simulation.

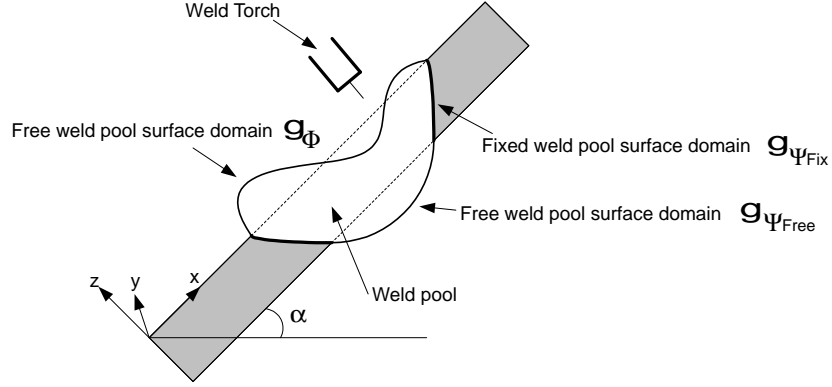


Figure 2: Sketch of the modelled situation of a work piece and its weld pool.

## 2.2 Surface deformation module

The surface deformation module calculates the deformation of the free surfaces in the weld pool for a hydrostatic situation [8]. It is necessary to consider the weld pool surface deformation in posture welding because the molten metal is influenced by gravity. (In top-down welding, simulating heat conduction may be sufficient [7].) The surface tension, gravity and arc pressure are considered. So the mathematical model describing the weld pool surface deformation is a system of two coupled non-linear PDEs, which arise from a balance between the internal pressure in the liquid and the counter pressure due to the surface tension and arc pressure. The two non-linear PDEs, each known as a *prescribed mean curvature equation*, respectively model the front and back free surface [8].

$$-\nabla \cdot \left( \frac{\gamma \nabla \Phi}{\sqrt{1 + |\nabla \Phi|^2}} \right) = f_\Phi(\Phi, x, y) + \lambda \quad \text{in } \mathcal{G}_\Phi, \quad (4)$$

$$-\nabla \cdot \left( \frac{\gamma \nabla \Psi}{\sqrt{1 + |\nabla \Psi|^2}} \right) = f_\Psi(\Psi, x, y) - \lambda \quad \text{in } \mathcal{G}_{\Psi_{\text{Free}}}. \quad (5)$$

In the above equations,  $\Phi$  represents deformation of the front weld pool surface,  $\Psi$  represents deformation of the back weld pool surface,  $\gamma$  represents the surface tension,  $\lambda$  represents a Lagrange multiplier,  $f_\Phi(\Phi, x, y)$  represents the pressure arising from gravity and arc pressure,  $f_\Psi(\Psi, x, y)$  represents the pressure arising from gravity.

The Lagrange multiplier  $\lambda$  is introduced into (4)-(5) due to a constraint on the surface deformation [13]. That is, mass conservation must be preserved, no matter material is added or not.

Figure 2 presents a sketch of the weld pool with naming of the weld pool surfaces. In this case,  $f_\Phi(\Phi, x, y)$  and  $f_\Psi(\Psi, x, y)$  can be expressed as:

$$f_\Phi(\Phi, x, y) = -P_a(x, y) - \rho g \sin \alpha x - \rho g \cos \alpha \Phi, \quad (6)$$

$$f_\Psi(\Psi, x, y) = \rho g \sin \alpha x + \rho g \cos \alpha (\Psi - s), \quad (7)$$

where  $P_a$  is the arc pressure and  $s$  is the thickness of the work piece [8].

The input to the surface deformation module includes the two-dimensional domains;  $\mathcal{G}_\Phi$  and  $\mathcal{G}_{\Psi_{\text{Free}}}$ , and a constraint on the surface deformation to conserve a mass balance between

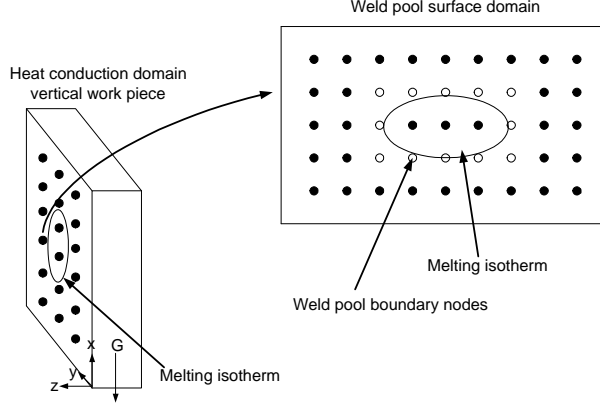


Figure 3: Extraction of the free weld pool surface domain approximated to the nodes of the surface deformation grid. Each node in the surface grid spatially corresponds to a point on the surface of the three-dimensional heat conduction domain.

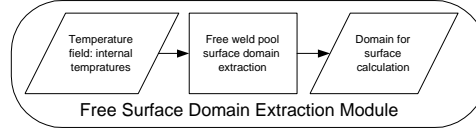


Figure 4: A diagram of the free surface domain extraction module, which shows input and output during simulation.

the change in the weld pool volume and the rate of filler material. The output includes the two-dimensional deformation fields:  $\Phi$  and  $\Psi$ . The right picture of Figure 1 shows a diagram of the surface deformation module.

### 2.3 Free surface domain extraction module

The free surface domain extraction module extracts the free weld pool surfaces  $\mathcal{G}_\Phi$  and  $\mathcal{G}_{\Psi_{\text{Free}}}$  using a given temperature field  $u$ . So the input to the module is  $u$  and the output is  $\mathcal{G}_\Phi$  and  $\mathcal{G}_{\Psi_{\text{Free}}}$ . The volume of the weld pool can be identified by locating the melting temperature isothermal; hence  $\mathcal{G}_\Phi$  and  $\mathcal{G}_{\Psi_{\text{Free}}}$  are defined by the intersection of the melting temperature isothermal and the surface of the three-dimensional heat conduction domain  $\Omega$ .

A simple approach to identifying the free surface domains and calculating the surface deformations is as follows. Take for instance the deformation of the front weld pool surface  $\Phi$ . A large enough rectangular two-dimensional finite element surface grid is built to cover  $\mathcal{G}_\Phi$  and some area around, see Figure 3. For each node point in the rectangular surface grid, the temperature can be found by interpolating the temperature field  $u$ . If the temperature at one node point of the rectangular surface grid is above the melting temperature, the node point “participates in” the finite element calculation of  $\Phi$  using (4); otherwise, the value of  $\Phi$  at the node point is simply enforced to a fixed value, e.g. zero. The advantage is that the work of constructing an unstructured finite element grid with curved boundaries can be saved. Of course, the accuracy of this simple “domain-embedding” approach depends on the grid resolution.

The free surface domain extraction module has the prescribed input and output as seen in Figure 4. Note that the input to the surface extraction module can be the output from the heat conduction module, while the output from the surface extraction module can be the input to the surface deformation module. Therefore, these three modules can be “coupled” in a sequence.

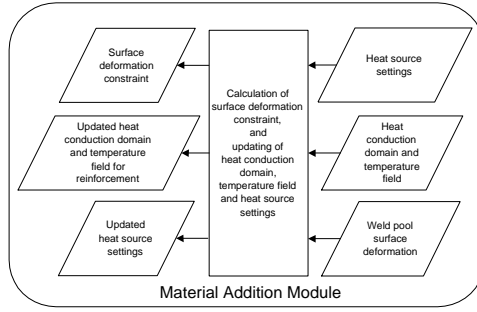


Figure 5: A diagram of the material addition module, which shows information input and output during simulation.

## 2.4 The material addition module

The material addition module calculates the addition of material to the work piece during the welding process; referred to as reinforcement of the work piece. As input, it takes heat source settings to calculate the reinforcement rate: e.g. rate of filler material and velocity. Additionally, it takes the weld pool surface deformation fields  $\Phi$  and  $\Psi$ , the heat conduction domain  $\Omega$  and the temperature field  $u$  to update  $\Omega$  and  $u$  with reinforcement material. The output from the material addition module is the updated  $\Omega$ , updated  $u$ , constraint on the surface deformation and updated heat source settings.

The material addition module has the prescribed input and output possibilities as seen in Figure 5. The input of the material addition module is the output from the heat conduction module, and vice versa. So these two modules can be “coupled together” to form a loop. Note that the possible use of the material addition module should not affect the internal implementation of the other three modules.

The material addition module does not solve PDEs, but mainly deals with geometrical changes in association with the reinforcement. These geometrical changes are not trivial options in the commercial finite element software. Therefore, this module demands most attention for future development.

### Update of the heat conduction domain

As described above, addition of material to the work piece results in a change in the three-dimensional domain  $\Omega$ . For a simulator using finite elements, this change in  $\Omega$  can be performed in different ways:

- Modify the existing grid by using alteration elements.
- Modify the existing grid by using relocation nodes.
- Extend the existing grid by adding new elements.

Modifying an existing grid with so-called alteration elements, as shown in Figure 6, Left, is a simple approach. Alteration elements are defined as those elements that freely can be “included in” or “excluded from” the calculations. More specifically, the heat conduction grid “occupies” in this case a volume that is larger than the actual work piece. This is because certain regions of the heat conduction grid consist of such alteration elements, which do not participate in the calculations initially. However, later on during a simulation, some of these alteration elements may be “turned on” to account for the material addition.

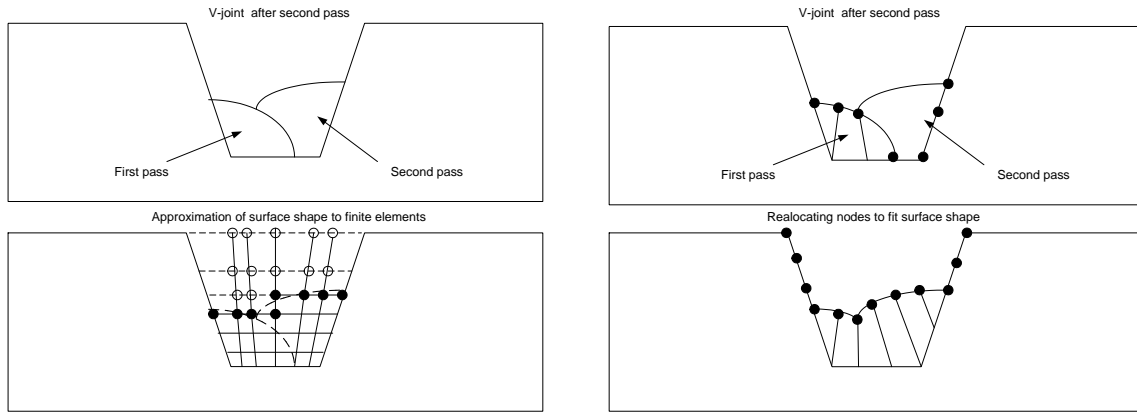


Figure 6: Left: A V-joint after second pass where the simulated reinforcement is fitted to nearest node. The alteration elements below the surface are “turned on”. Right: A V-joint after second pass where the simulated reinforcement is approximated by reallocating nodes followed, if necessary, by grid refinement by means of an adaptive grid algorithm.

This change is needed because the alteration elements have been deliberately placed where reinforcement may take place during the welding process. Before filler material is added, the alteration elements represent air and afterwards represent work piece material; indicated by letting the state of the alteration elements change from “turned off” to “turned on”. When the alteration elements are “turned off” and represent air, they are actually placed outside the domain of the “real work piece. This means that they should behave as if the ordinary boundary conditions are enforced during the simulation. The heat transport in the weld seam in front of the heat source has a very limited effect on the temperature distribution, because the material in front of the heat source is close to the initial temperature. The properties of “turned off” alteration elements should then have none or limited influence on the calculation of temperature distribution. During a simulation, alteration elements are “turned on” to simulate addition of liquid material. This is done by setting their properties equal to the base material and by setting their temperature equal to the temperature of the droplets of liquid metal entering the weld pool during the welding process.

Alteration elements are included into the grid from the beginning, which entails that the maximum magnitude of the reinforcement should be known prior to the simulation such that the distribution of nodes can reflect the expected shape. The resolution of alteration elements should be sufficiently fine to be able to approximate the reinforcement shape sufficiently. The left picture of Figure 6 sketches a V-joint after a second pass, where reinforcement is approximated to the nearest node. Elements inside the reinforcement are turned on.

Modifying an existing grid by with reallocation nodes is a more complicated procedure but it has the advantage that no alteration elements are included, which can affect the calculations, because of the alteration elements approximated behaviour as air when they are turned off. The main advantage is, however, that the maximum magnitude of the reinforcement does not have to be known prior to the simulation. Instead it can be obtained from the surface deformation module, which enables a more precise simulation of complex reinforcement shapes. This is because the relocation nodes are following the changes in the boundary of the work pieces region  $\Omega$  with material addition instead of approximating the surface shape as with alteration elements. The right picture of Figure 6 sketches a V-joint after second pass, where the reinforcement is approximated by relocation nodes. When moving nodes in the finite element grid the finite elements will be deformed. It is only possible to a certain extent in order to avoid

large errors in the calculation. Therefore, this procedure should be coupled with an adaptive grid procedure to regenerate the grid.

A hybrid of the two methods can also be used to avoid too many adaptive grid iterations. Alteration elements are allocated in the grid and then the nodes near the surface of the reinforcement are moved to give a better approximation. In this case it will not be the same nodes, which are moved and, therefore, the deformation of each element will be limited.

Extending the existing grid by adding new elements entails a rebuilding of the laid out grid and, hence, a re-allocation of data storage for the system of algebraic equations, which the finite element method utilises. This rebuilding gives full freedom to adapt to any change in the heat conduction domain. However, this method demands a flexible grid generation utility, which can re-generate a grid based on information about the reinforcement of the heat conduction domain.

## **2.5 Implementation of modules**

All the four modules in the architecture are implemented as objects, using the object-oriented programming approach of Diffpack. This enables a separate development of the numerical solvers inside the heat conduction module and the weld pool surface deformation module. Additionally, the modules are not confined to a particular numerical method. Object orientation also makes it easy to build a hierarchy of different heat conduction modules (or a hierarchy of surface deformation modules) with different internal numerical schemes. An important programming technique is to equip each hierarchy of modules with a unified “input-output interface”, which is compatible with those of other hierarchies. Such a unified interface should clearly be made independent of the internal solution method. Therefore, in cases where a certain implementation of a module is inadequate it can be replaced. This is of special interest for the material addition module because it is a non-trivial task in finite element simulations and, therefore, the material addition module will very likely be subject to further development. All things considered, this enables a fast, easy and continuing development of a simulation system.

## **3 System configuration**

Different configurations of the simulation system can affect its usability for different welding applications. Therefore, requirements to the simulation system from the chosen welding application need to be considered carefully before configuring the simulation system. Table 1 gives an overview of the minimum demands from different welding applications. All GMAW processes are regarded to have full penetration at least in the root pass, which means that there will be a free surface on the back side of the work piece. Table 2 gives overview of different geometrical weld quality variables. The table indicates which module is the main module and therefore necessary for generating information about the particular weld quality variable. The subsequent sections describe the different system configurations.

### **3.1 Configuration I**

Use of only the heat conduction module results in a simulation system, which contains information about the thermal history but no information about material addition or weld surface deformation. Such a system is usable for top-down Gas Tungsten Arc Welding (GTAW or TIG) without material addition on horizontal work piece without full penetration. In this case

Table 1: List of minimum demands from different welding applications to the configuration of the simulator. Feedback under material addition refers to feedback from the surface deformation module used for updating the heat conduction domain.

No.	Welding type	Module			Material addition	
		Heat Conduction	Surface deformation and Extraction	Material Addition	No Feedback	Feedback
I	GTAW top-down, ÷ material addition, ÷ full penetration	x				
II	GTAW top-down, ÷ material addition, full penetration	x	x			
II	GTAW postural, ÷ material addition	x	x			
III	GTAW, top down / postural, single pass, material addition	x	x	x	x	
IV	GTAW, top down / postural, multi pass, material addition	x	x	x	x	
III	GMAW, top down / postural, single pass	x	x	x	x	
IV	GMAW, top down / postural, multi pass	x	x	x		x

Table 2: List of different geometrical weld quality variables. The table indicates which module is the main module for generating information about the particular variable. The material addition module is necessary for the heat conduction module when simulation a welding process with material addition to obtain the right thermal distribution and thermal history.

Weld quality variable	Driven by module		
	Heat Conduction	Surface deformation and Extraction	Material Addition
Penetration / Fusion	x		(x)
Notch / Undercut		x	
Unstable weld pool		x	
$\Delta t_{8,5}$	x		(x)

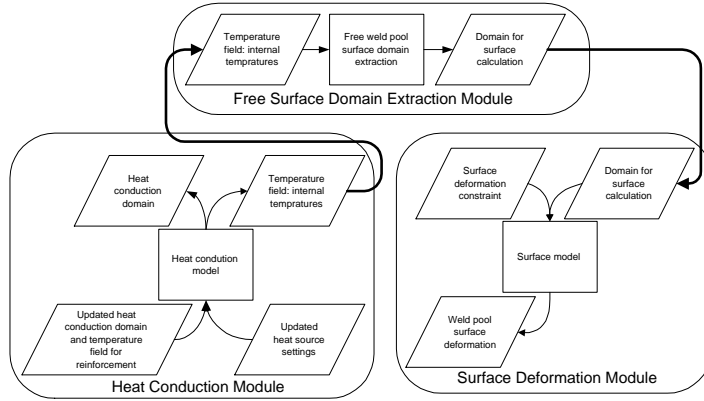


Figure 7: Diagram of configuration II; a simulation system for heat conduction and surface deformation simulation.

the weld pool bottom supports the weld pool. A small inclination of the work piece can be allowed such that the well pool bottom can still support the weld pool. The system will be able to simulate the weld quality variables: penetration / fusion of the work piece and  $\Delta t_{8,5}$ .

### 3.2 Configuration II

A simulator system, which includes the heat conduction, the surface deformation and the free surface domain extraction modules, extends the previous configuration with information on weld pool surface deformation. This configuration allows an inclination of the work piece and full penetration welding, because it is possible to simulate weld pool surface deformation and, hence, to identify if the weld pool surface breaks and destroys the weld. The system is still limited to GTAW without material addition, because material addition is not included. The system will be able to simulate the weld quality parameters: penetration / fusion of the work piece,  $\Delta t_{8,5}$ , undercut / notch and unstable weld pool surfaces.

The configuration of the simulation system is shown in Figure 7. The heat conduction module transfers the temperature field to the free surface domain extraction module. The surface extraction module determines the free surface domain and passes that on to the surface deformation module. The output from the surface deformation module is used only as simulation result and not for further calculation inside the simulation system.

### 3.3 Configurations III and IV

A simulator including all the four modules can be configured in two different ways, depending on whether the surface deformation is used for updating  $\Omega$  or not. The first configuration uses no feedback from the surface deformation module and the second configuration uses the feedback. These two different configurations give different simulation capabilities of a welding application.

#### 3.3.1 Configuration III

The coupling of the material addition module with the heat conduction module for the case of no feedback from the surface deformation module can be seen in Figure 8. The change from configuration II is the inclusion of material addition. The material addition module receives the heat conduction domain and the temperature field for update with reinforcement

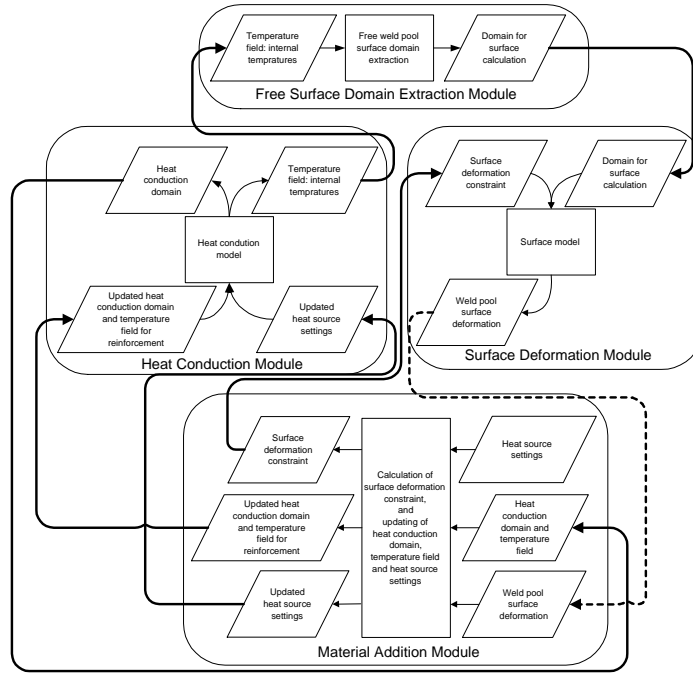


Figure 8: Diagram of configuration III and IV; a system for simulating heat conduction, surface deformation and material addition. In configuration III, the surface deformation is not used for calculating the shape of reinforcement, whereas it is used in configuration IV. The difference is represented by the dotted line.

material. Reinforcement material update is the basic task of the material addition module. The material addition module supplies the surface deformation module with a surface deformation constraint. A possible surface deformation constraint can be calculated on the basis of the difference between the necessary reinforcement rate, which can be calculated from the cross-sectional area of the gap and the welding speed, and the volume rate of reinforcement material, which is calculated from the wire feed speed and wire diameter. An excessive volume of reinforcement material will result in a bulb on the surface of the work piece. Therefore, the amount of excessive volume is passed on to the surface module as a constraint on the change in volume with deformation of the free weld pool surface [8]. This configuration enables modelling of gas metal arc welding (GMAW or MIG/MAG) and GTAW both with full penetration and inclination of the work piece. However, the configuration implies that the final shape of reinforcement is known to a satisfactory level a priori, because the shape of the surface deformation is not passed on to the material addition module for reinforcement calculations. Therefore, this configuration of the simulation system is useful for work piece geometries where single pass welding is usable, e.g., thin plate I-joint, V-joint or T-joint. In these cases, the error in the temperature distribution is limited when approximating the change in the heat conduction domain by a qualified guess. For single pass welding, the heat source settings should be chosen so the weld seam is filled in a single pass. This entails that the welding speed is set on the basis of the rate of filler material or vice versa.

The system will be able to simulate the weld quality parameters: penetration / fusion of the work piece,  $\Delta t_{8,5}$ , undercut / notch and unstable weld pool surfaces.

### 3.3.2 Configuration IV

The coupling of the material addition module with both the heat conduction and surface deformation modules for the case of feedback from the surface deformation module can be seen in Figure 8. The only change from configuration III is surface deformation feedback to the material addition module represented by the dotted line. This information enables the material addition to reflect the shape of the surface deformation in the reinforcement of the heat conduction domain. This is of special interest for multi pass welding, because the configuration of a new layer of reinforcement material is dependent on the configuration of previous layers. This is a result of the relatively large change in the weld seam geometry during the welding process. Additionally, the configuration of a new layer of reinforcement material is dependent on the temperature distribution in the weld seam, which also depends on the geometrical change of the weld seam with reinforcement. This configuration allows GMAW with full penetration and inclination of the work piece usable for multi pass welding of e.g. I-joints, V-joints, U-joints or T-joints.

The system will be able to simulate the weld quality parameters: penetration / fusion of the work piece,  $\Delta t_{8,5}$ , undercut / notch and unstable weld pool surfaces.

## 4 Numerical solution method

Different numerical solution methods are used for the heat conduction and the surface deformation modules to be able to conduct a sound and fast simulation. The object-oriented approach, supported by Diffpack, enables separate development and testing of the solvers without depending on other modules. This results in an easier development. The following text presents the used numerical strategies inside the two modules.

### 4.1 Numerical method for the heat conduction equation

The material properties of heat capacity and conductivity are considered temperature dependent, whereas the density is regarded temperature independent. The temperature dependencies result in a non-linear PDE, which requires a non-linear solver. The iterative solution method Successive Substitution is used, because it is simple and because it gives in this case sufficiently good convergence rates. At each time step, the Successive Substitution solves a non-linear system of algebraic equations. So an iterative procedure is carried out at every time step, see (8). The iteration is repeated until the change in the solution between two iterations is sufficiently small. The solution of the linear system of algebraic equations in each iteration uses the conjugated gradient method, which utilises that the fact the system matrix is sparse, symmetric and positive definite.

$$\mathbf{A}(\mathbf{u}^k)\mathbf{u}^{k+1} = \mathbf{b}(\mathbf{u}^k) \quad k = 1, 2, \dots \quad (8)$$

The temperature field  $u$  normally has large gradients and moves along with the heat source. Therefore, a high grid resolution is needed along the weld seam to avoid large numerical errors. A uniformly high grid resolution throughout  $\Omega$  requires a large computational effort. However, material a short distance in front of the heat source will almost always have initial temperatures and, hence, temperature gradients in front of the heat source are very large. How far in front of the heat source this is the case depends on the welding speed and the conductivity of the metal. Additionally, the gradients behind the heat source are relatively small because of the slow cooling of the work piece. The change in the value of the temperature gradients indicates

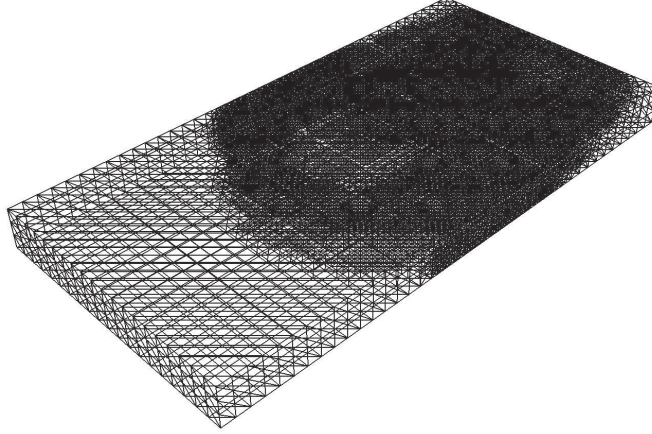


Figure 9: A snapshot of the grid of the work piece during a simulation. An adaptive algorithm is used to refine the elements around the heat source.

that very fine elements are only needed close to the heat source and its tail. The rest of the grid elements can be coarser. For small welding simulations the penalty of not using adaptive grid algorithms can be insignificant, but for larger welding simulations difference in grid density can save an significant amount of computational effort [12]. The heat conduction module is used for all sizes of work piece and, therefore, an adaptive grid algorithm is used. Figure 9 shows a grid where the adaptive refinement algorithm is used.

## 4.2 Numerical method for the surface deformation equation

The PDEs describing the surface deformation ((4) and (5)) are non-linear. This again calls for a non-linear solver and the Newton-Raphson method can be chosen in this case. Take  $\Phi$  for instance, the Newton-Raphson method can be summarised as the following iteration:

$$\mathbf{J}(\Phi^k)\delta\mathbf{u}^{k+1} = -\mathbf{f}(\Phi^k), \quad (9)$$

$$\Phi^{k+1} = \Phi^k + \delta\Phi^{k+1}, \quad (10)$$

where  $\mathbf{J}$  is the Jacobi matrix and  $\mathbf{f}$  is the right-hand side vector associated with a Newton-Raphson formulation of (4), see e.g. [9].

The iterative process continues until the change in the solution between two iterations is sufficiently small. Again, the solution of the linear system of algebraic equations, see (9), can use the conjugated gradient method.

The PDEs describing the surface deformation are connected by an unknown  $\lambda$ , such that the solutions  $\Phi$  and  $\Psi$  together fulfil a mass conservation constraint [8]. The associated volume criterion defines a function dependent on  $\lambda$ . An example is the following equation, which calculates the deviation in the weld pool volume:

$$dV(\lambda) = \int_{\mathcal{G}_\Phi} \Phi(x, y, \lambda) dx dy - \int_{\mathcal{G}_\Psi} \Psi(x, y, \lambda) dx dy, \quad (11)$$

which should satisfy the condition:  $dV(\lambda) = dV_{\text{desired}}$ .

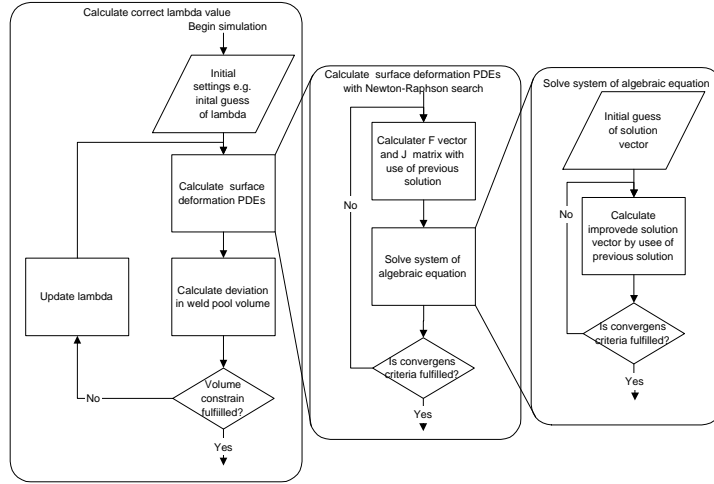


Figure 10: Sketch of the three needed iterations loops to solve the weld pool surface deformation PDEs.

Therefore, it cannot be expected that any value of  $\lambda$  is usable, and the objective is then to identify  $\lambda^*$  so that the deviation is equal to a desired deviation, e.g., zero. A Secant-type method (see [6]) can be used to find an approximation to  $\lambda^*$ . The solution scheme is as follows:

1. Start with a first initial guess  $\lambda_1$ . Solve equations (4) and (5) using  $\lambda_1$  and compute  $dV(\lambda_1)$  by numerical integration. If  $|dV(\lambda_1) - dV_{\text{desired}}|$  is sufficiently small, then we have found  $\lambda^* = \lambda_1$ , else continue.
2. Choose a second initial guess  $\lambda_2$ . Solve equations (4) and (5) using  $\lambda_2$  and compute  $dV(\lambda_2)$  by numerical integration. If  $|dV(\lambda_2) - dV_{\text{desired}}|$  is sufficiently small, then we have found  $\lambda^* = \lambda_2$ , else continue.
3. For  $n = 3, 4, \dots$ , repeat the following steps until  $|dV(\lambda_n) - dV_{\text{desired}}|$  is sufficiently small:

- Compute a new value of  $\lambda_n$  by

$$s = \frac{dV(\lambda_{n-1}) - dV(\lambda_{n-2})}{\lambda_{n-1} - \lambda_{n-2}},$$

$$\lambda_n = \lambda_{n-1} - \frac{(dV(\lambda_{n-1}) - dV_{\text{desired}})}{s}.$$

- Solve (4) and (5) using  $\lambda_n$  and compute the  $dV(\lambda_n)$  by numerical integration.

Note that the above numerical strategy calls for three levels of iterations, see Figure 10. In the implementation, the surface deformation module uses internally two nonlinear PDE solver objects, one for (4) and the other for (5). The topmost iteration is implemented in the surface deformation module to find an approximation to  $\lambda^*$  that fulfils the volume constraint.

## 5 Vertical I-joint GMAW simulator

To demonstrate the architectural principle, this section presents the configuration and results from a vertical falling single pass thin sheet I-joint GMA welding simulation. A sketch of the welding application can be seen in Figure 11.

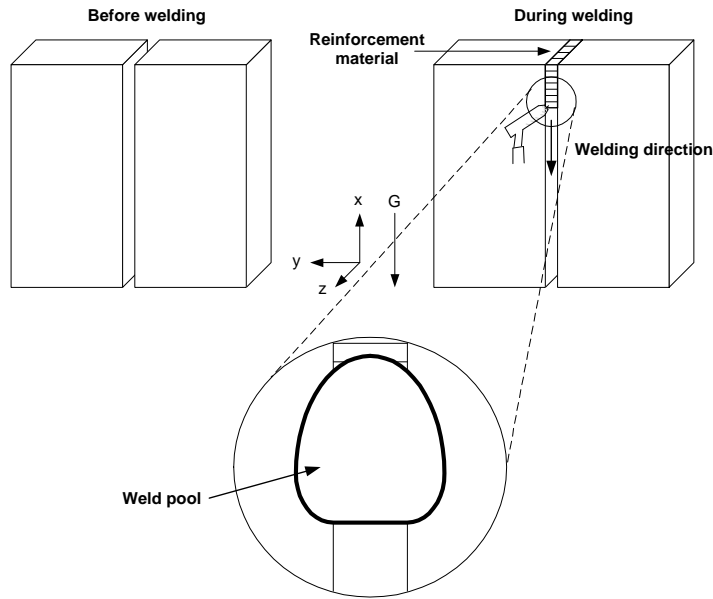


Figure 11: Sketch of a vertical falling I-joint GMA welding situation of 3 mm sheets, which is conducted in a single pass. The front of the weld pool is sketched as a straight line. This is due to the implementation of material addition where the new material is added as rectangular blocks.

## 5.1 Configuration

The configuration involves all the four modules, but without feedback from the surface deformation module to the material addition module, i.e., configuration III.

The most interesting module in the simulator system is the material addition module because of its task of reinforcement calculation, which is non-trivial for the finite element simulations. Therefore, its implementation in the present simulator is described. No feedback of surface deformation is assumed, because the welding process can be performed in a single pass. The bulb of reinforcement material that appears on the front and back sides of the work piece has insignificant influence on the overall temperature distribution in the work piece. Therefore, this is disregarded when adding filler material to the heat conduction domain  $\Omega$ . Instead, a filler material efficiency factor is used to account for the volume outside heat conduction domain  $\Omega$ .

The material addition module is chosen to simulate material addition by use of alteration elements because it is the simplest approach. A schematic view of the implementation of the material addition module can be seen in Figure 12. The material addition function addresses two objects from the heat conduction module; the heat conduction domain grid and the internal temperature field. The heat conduction domain grid is updated with information on which alteration elements are turned on. The area of turned-on elements changes their temperature in the internal temperature field from initial temperature to the temperature of droplets of liquid metal entering the weld pool. Additionally, the material addition module calculates the excessive volume of reinforcement material, which makes a bulb on the work piece. This excessive volume rate of reinforcement material is used to set up a constraint on the surface deformation. In the process of determination of the reinforcement, the material addition module also needs to be able to change the heat source settings to secure that the weld seam is filled in a single pass as wanted. The heat input is also updated so the energy used to heat up the filler material is deduced from the heat input coming from the arc.

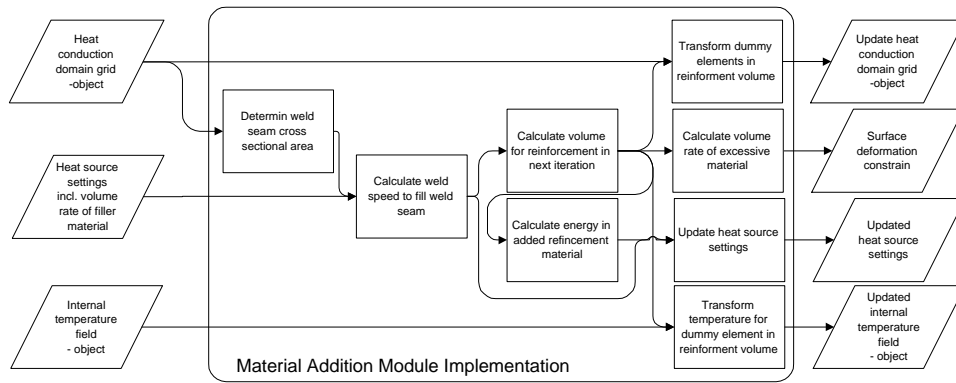


Figure 12: Diagram of implementation of the material addition module at programming level.

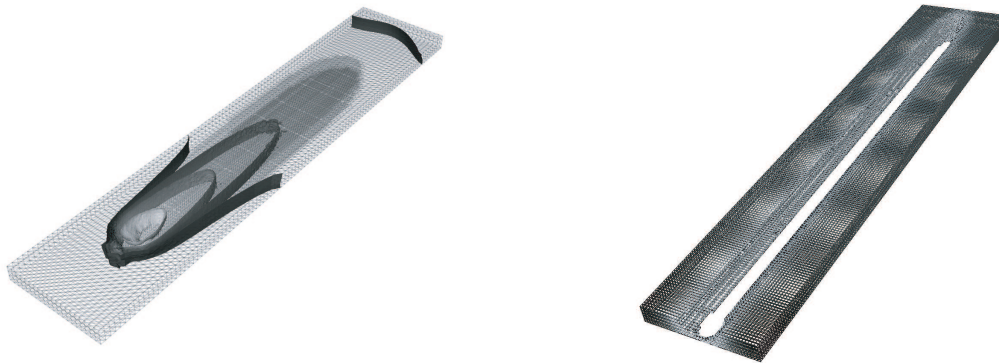
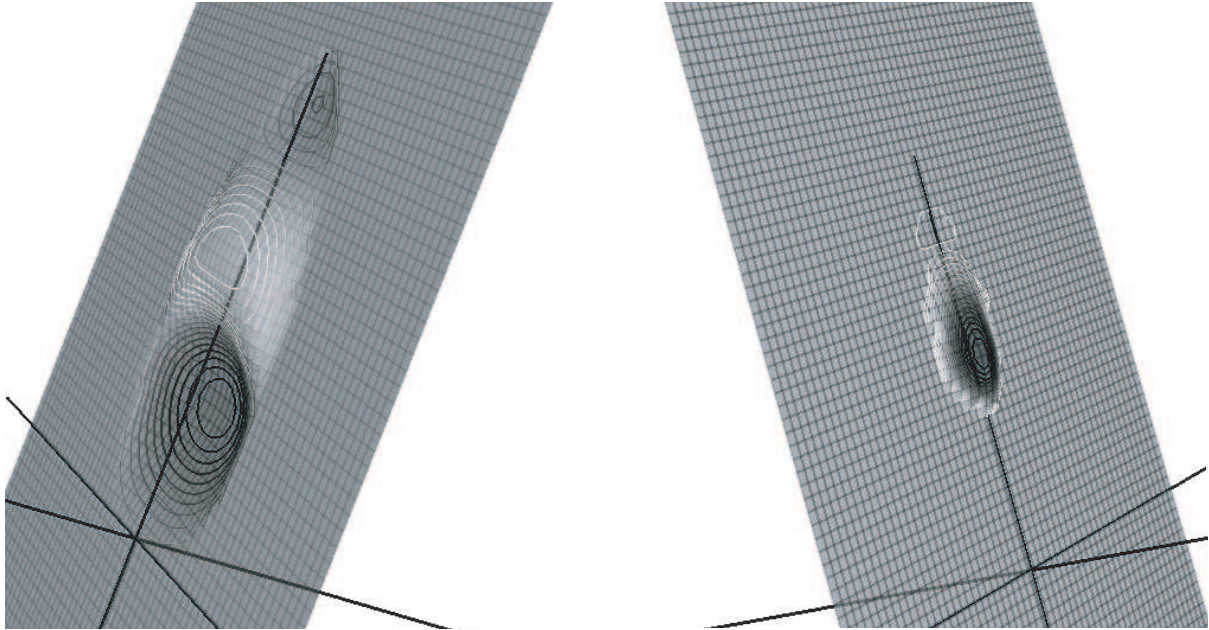


Figure 13: Left: Temperature distribution in the heat conduction domain. The isothermals are set at: 700 °C, 900 °C, 1100 °C and 1530 °C. Right: Fusion of the work pieces is shown by removing all elements, which have been above the melting point. It shows that a full penetration welding is obtained except from the start of the welding. At the end of the welding the weld pool gets wider because the heat input is not able to be conducted away from the fusion zone.

## 5.2 Simulation results

Results from a simulation can be viewed in Figures 13 and 14. The work piece is 100 mm long, 40 mm broad and 3 mm thick. The left picture of Figure 13 shows the temperature distribution in the heat conduction domain by use of four isothermals: 700°C, 900°C, 1100°C and 1530°C. The last one is the melting point of the metal and, therefore, the 1530°C isothermal identifies the boundary of the weld pool. Note that the picture also reveals the adaptive grid used.

The fusion of the work piece and the penetration can be identified in the right picture of Figure 13, which shows a reference grid containing the maximum temperatures obtained during simulation. All the elements in the grid having temperatures above the melting point are removed. It can be seen that full penetration does not occur initially. Therefore, the energy input needs to be higher in the beginning to obtain full penetration from the start of the welding. It can also be seen that at the end of the welding process, the weld pool is getting wider in the bottom before the heat source is turned off. This is because the energy cannot be conducted away from the fusion zone at the end of the work piece. This increases the risk of breaking



*Figure 14: The surface deformation. The left picture shows the surface deformation  $\Phi$  for the front surface  $\mathcal{G}_\Phi$  and the right shows deformation  $\Psi$  for the back surface  $\mathcal{G}_\Psi$ . The heat source is moving from the top and down. The centre of the heat source is located at the origin of the coordinate system.*

the weld pool surface. To avoid this, the heat input should be reduced close to the end of the welding process.

Figure 14 shows the surface deformation. The left picture shows the front surface deformation  $\Phi$ . The centre of the heat source is located at the origin of the coordinate system. The effect of the arc pressure can be seen as a depression on the surface. The right picture shows the back surface deformation  $\Psi$ . The simulation results show that the simulator works quite well. However, the simulation results are not usable for process prediction before the heat source and material addition function are calibrated to experiments for chosen process settings. The simulator can then be used to predict the welding process at different process settings by an interpolation between the known process settings.

## 6 Results and discussion

The presented general architecture for the welding simulation systems consists of four basic modules; heat conduction module, free surface domain extractor, surface deformation module and material addition module. Different configurations of the simulation system results in different simulation capabilities; from top-down bead-on-plate gas tungsten arc welding, where using only the heat conduction module is sufficient, to multi pass postural GMAW of complex seams, where all the four modules are needed.

The architectural principle has been demonstrated by configuring a simulator for vertical I-joint single pass GMAW. This configuration uses the four modules that are implemented as objects in Diffpack, allowing a separated development of each module and an easy configuration of the simulation system.

This architecture has been developed without depending on the details of how each module handles its specific task. Therefore, different approaches can be used inside each module

as long as the interface to other modules is preserved. As examples of future work, a more advanced heat source suitable for curved geometries can be developed and implemented in the heat conduction module. The material addition module can be extended with more advanced algorithms for adding reinforcement material. However, these developments can be implemented inside each module without interfering with other modules and, therefore, it is easy to extend the simulation system as the demands from the welding applications appear. Therefore, this architecture has been found usable for an ongoing project to develop an automated off-line welding programming system.

## Acknowledgement

M.Sc., PhD Student C. Terp, Department of Production, Aalborg University, Denmark is acknowledged for many inspiring discussions and for providing heat source calibration information. Additionally, Odense Steel shipyard A/S and the Danish Academy of Technical Science are acknowledged for the financial support, which makes this research project possible.

## References

- [1] Z. N. Cao and P. Dong. Modelling of gma weld pools with consideration of droplet impact. *Journal of Engineering Materials and Technology, Transactions of the ASME*, 120(4):313–320, 1998.
- [2] M. Dassisti, L. M. Galantucci, and A. Caruso. The use of three-dimensional finite element analysis in optimising processing sequence of synergic mig welding for robotic welding system. In *Advanced Manufacturing Systems and Technology*, pages 585–592. Springer-Verlag, 1996.
- [3] Diffpack Home Page. <http://www.nobjects.com/diffpack>.
- [4] J. Goldak, A. Chakravarti, and M. Bibby. A new finite element model for welding heat source. *Metallurgical Transactions B*, 15B(2):299–305, 1984.
- [5] M. Gu, J. Goldak, and E. Hughes. Steady state thermal analysis of welds with filler metal addition. *Canadian Metallurgical Quarterly*, 32(1):49–55, 1993.
- [6] Joe D. Hoffman. *Numerical Methods for Engineers and Scientists*. Marcel Dekker, 2nd edition, 2001.
- [7] H. Holm, P. V. Jeberg, and C. Bro. Application of numerical model for off-line programming of posture robot welding. In *Proceedings of 12th International TWI Computer Technology in Welding and Manufacturing Conference, 27-30 August 2002, Sydney*, page paper no. 81, 2002.
- [8] P. V. Jeberg and H. Holm. 2d weld pool surface model in 3d space with one degree of freedom and its theoretical limitations for weld planning. In *Proceedings of International Conference on Productive Welding in Industrial Applications, 20-22 May 2003, Lappentanta, Finland*, 2003.

- [9] H. P. Langtangen. *Computational Partial Differential Equations - Numerical Methods and Diffpack Programming*. Textbooks in Computational Science and Engineering. Springer Verlag, 2nd edition, 2003.
- [10] A. F. Mills. *Heat and Mass Transfer*. Irwin, 1st edition, 1995.
- [11] T. Ohij, A. Ohkubo, and K. Nishiguchi. Mathematical modelling of molten pool in arc welding. In *Mechanical Effects of Welding*, pages 207–214. Springer-Verlag, 1991.
- [12] S. M. Roberts, H. J. Stone, D. Dye, and R. C. Reed. Computer modelling of welding, review of current best practice. Technical report, Department of Material Science and Metallurgy, University of Cambridge, UK, 1999.
- [13] F. Y. M. Wan. *Introduction to the Calculus of Variations and its Applications*. Chapman and Hall, 1st edition, 1995.
- [14] D. Weiss, J. Schmidt, and U. Franz. A model of temperature distribution and weld pool deformation during arc welding. In *Mathematical Modelling of Weld Phenomena 2*, pages 22–39. Institute of Materials, 1995.